

## Title

Assessment of a Nano-Docetaxel Combined Treatment for Head and Neck Cancer

## Running Title

Nano-Docetaxel Combination treatment

## Authors names and affiliations

Gee Young Lee<sup>1,2</sup>, Mohamed Mubasher<sup>3</sup>, Tamra S. McKenzie<sup>1,4</sup>, Nicole C. Schmitt<sup>5</sup>, Merry E. Sebelik<sup>4,5</sup>, Carrie E. Flanagan<sup>4,5</sup>, Maya B. Cothran<sup>6</sup> and Hadiyah N. Green<sup>1,2,6\*</sup>

<sup>1</sup>Department of Surgery, Morehouse School of Medicine, 720 Westview Drive, Atlanta, GA 30310, USA

<sup>2</sup>Biomedical Laboratory Research & Development Service, Department of Veterans Affairs, Office of Research and Development, Birmingham VA Medical Center, 700 19<sup>th</sup> Street, Birmingham, AL 35233, USA

<sup>3</sup>Community Health and Preventive Medicine, Morehouse School of Medicine, 720 Westview Drive, Atlanta, GA 30310, USA

<sup>4</sup>Atlanta VA Medical Center, Atlanta VA Health Care System, 1670 Clairmont Road, Decatur, GA 30033, USA

<sup>5</sup>Department of Otolaryngology – Head and Neck Surgery, Emory University School of Medicine, 550 Peachtree Road NE, Atlanta, GA 30308, USA

<sup>6</sup>Ora Lee Smith Cancer Research Foundation, Advanced Technology and Development Center, 75 5<sup>th</sup> Street NW, Atlanta, GA 30308, USA

## Corresponding author

Hadiyah N. Green, Ph.D.

Department of Surgery, Morehouse School of Medicine

720 Westview Drive, Atlanta, GA 30310, USA

+1 (256) 457-5411

[hgreen@msm.edu](mailto:hgreen@msm.edu) or [drgreen@oralee.org](mailto:drgreen@oralee.org)

## ABSTRACT

**Objective:** The combination of docetaxel (DTX) with Laser-Activated NanoTherapy (LANT), as a treatment for head and neck cancer (HNC) may enhance the therapeutic efficacy of lower doses of DTX, thereby minimizing the effective dosage, side effects and treatment times.

**Material and methods:** Three HNSCC cell lines, Detroit 562, FaDu, and CAL 27, were treated with four combinations of DTX + LANT to evaluate DTX dose reduction and cell viability.

**Results:** The 1 nM DTX + 5 nM LANT combination was the most effective treatment, increasing cell death over its corresponding DTX monotreatment with approximately 86.6%, 80.7%, and 92.1% cell death for Detroit 562, FaDu, and CAL 27, respectively. In Detroit 562, the 1 nM DTX + 5 nM LANT combination treatment resulted in the highest percentage of DTX dose reduction at 84.6%; in FaDu and CAL 27, the 0.5 nM DTX + 5 nM LANT combination treatment resulted in the highest percentage of DTX dose reduction at 78.2% and 82.4%, respectively.

**Conclusion:** LANT may increase the therapeutic efficacy of DTX at significantly lower doses, which could improve patient outcomes.

## KEYWORDS

docetaxel, combination therapy, nanoparticles, head and neck squamous cell carcinoma, oncology, therapies

## 1 INTRODUCTION

Head and neck cancers (HNC) have a poor prognosis with a worldwide 5-year survival rate of less than 50% [1-3], and head and neck squamous cell carcinomas (HNSCC) constitute 90% of these cases [4]. Many HNC patients present with locally advanced, difficult-to-treat, inoperable, recurrent, or drug-resistant tumors [1-7]. Docetaxel (DTX) is an anticancer drug that disrupts normal microtubule functioning during the cell cycle. It inhibits interphase and mitosis by promoting and stabilizing microtubule assembly, which prevents microtubule depolymerization, making the G2/M transition impossible [8,9]. This mechanism limits cell growth in the locoregional area of the tumor. However, DTX is also associated with adverse effects that may be severe or dose-limiting, including febrile neutropenia, neuropathy, and alopecia [10].

The scientific community is beginning to explore strategies to shift the therapeutic window and reduce the effective dose of DTX to limit complications by combining DTX with other treatment modalities and/or manipulating the dosing schedule [7,11]. For locally advanced HNSCC, DTX is paired concurrently with other chemotherapeutic drugs. The established dose for this cancer type is 75 mg/m<sup>2</sup> when administered with cisplatin and fluorouracil at varying dosages and schedules depending on the subsequent treatments such as radiation or chemotherapy [12-15]. Studies combining DTX with other

chemotherapeutic drugs and varying the DTX dosage and delivery have shown great potential in decreasing side effects [13,16,17].

Nanoparticles and nanomaterials have shown to be promising anti-cancer therapeutics alone and in combination with chemotherapeutic agents. These nanomedicines have demonstrated dramatic improvement in tumor targeting and therapeutic efficacy when used in drug delivery systems, radiotherapy, and photothermal or photodynamic therapy [18-24]. Many nano-based approaches have been combined with DTX to enhance targeted drug delivery and tumor specificity, consequently minimizing side effects [17,25-31]. Photothermal therapies utilizing nanoparticles and laser light have shown success in tumor treatment *in vitro* and *in vivo* as a site-specific ablative approach rather than theranostic drug delivery [32,33]. Our work focuses on a particular class of laser-activated nanoparticles, specifically, a thermal ablation platform treatment using near-infrared excitation of gold nanorods (AuNRs), known as Laser-Activated NanoTherapy (LANT) [Figure 1]. This LANT platform is not designed to enhance targeting but specifically to induce loco-regional cell death at the site of laser-activation for the sole purpose of its thermal ablation and therapeutic effect. Our prior work with LANT as a single modality has demonstrated ~100% cell death *in vitro* ( $p < 0.0001$ ) and ~100% tumor regression *in vivo* ( $p < 0.0001$ ) with no observable toxicities [33,34]. However, to our knowledge, no such platform has been approved by the US Food and Drug Administration (FDA) for use in humans. LANT presents an opportunity to override some of the physiologic obstacles encountered within the tumor microenvironment and with DTX specificity. The present study investigates how LANT, as part of a combination treatment regimen, enhances the therapeutic efficacy of lower doses of DTX for treating three head and neck squamous cell carcinoma (HNSCC) cell lines.

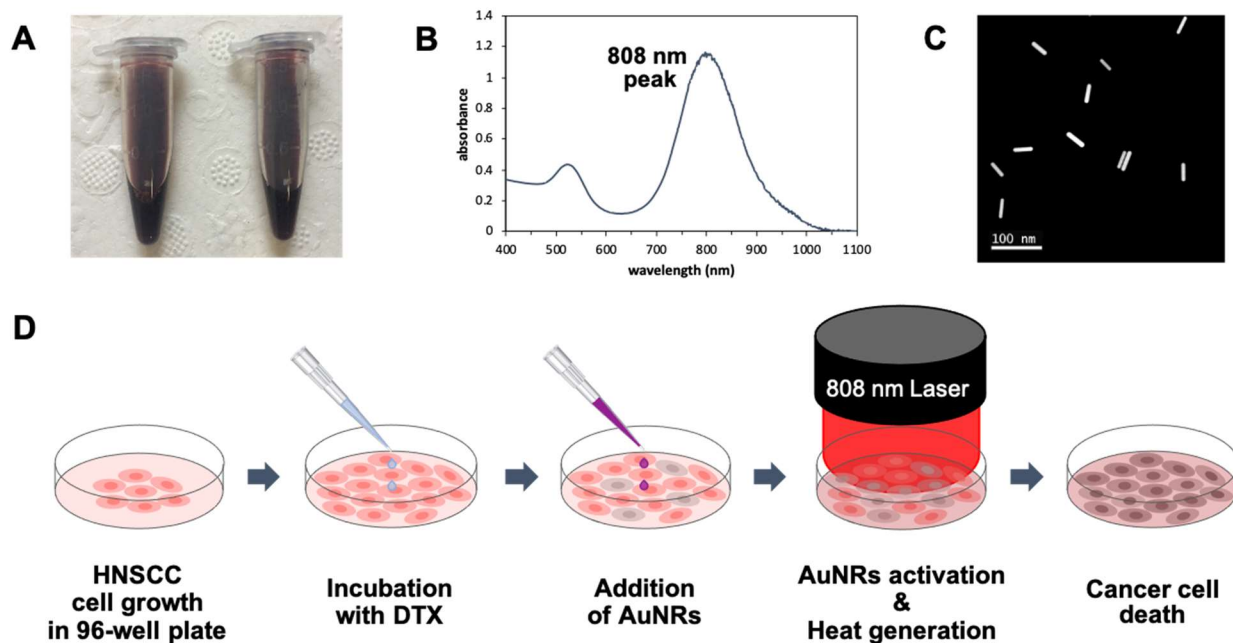


**Figure 1.** (A) PEGylated AuNRs solution utilized in Laser-Activated Nanotherapy (LANT), (B) UV-VIS-NIR spectrum of AuNRs showing an 808 nm absorption peak, (C) STEM image of a AuNRs having 40 nm in length, 10 nm in width, and aspect ratio ( $R = 4$ ), and (D) schematic illustration of DTX and LANT combination treatment *in vitro*. The illustration demonstrates one well of a 96-well plate.

## 2 RESULTS

### 2.1 Cell Death Effects of LANT Monotreatment

The *in vitro* effects of LANT as a monotreatment (percentage of cell death, dose-response curves, and half-maximal effective concentrations (EC<sub>50</sub>) of 8.1 nM, 11.0 nM, and 6.7 nM) were previously established for Detroit 562, FaDu, and CAL 27, respectively [37,39]. In summary, 4 min NIR laser excitation of AuNRs at six concentrations (0, 5, 10, 15, 20, and 25 nM) demonstrates AuNR concentration-dependent cell death [Figure 2]. LANT induced significant cell death in all three HNSCC cell lines, with increasing AuNR concentration directly increasing the percentage of cell death. Consistent with our previous findings [33], LANT doses of 25 nM induced approximately 100% cell death ( $p < 0.0001$ ) in all three HNSCC cell lines.

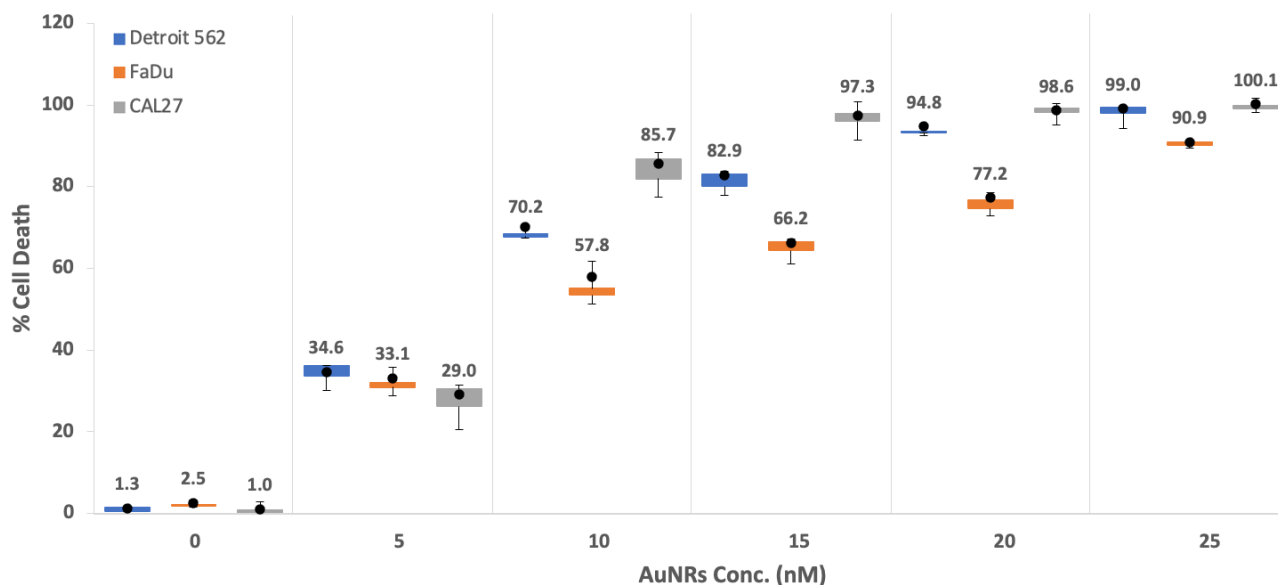


**Figure 2.** Box and Whisker plot to display LANT monotreatment dose-response with AuNRs concentration for HNSCC cell lines: Detroit 562 (blue box), FaDu (orange box), and CAL 27 (gray box) at concentrations of 0, 5, 10, 20, and 25 nM; 25  $\mu$ L of AuNRs per well, with and without 808 nm NIR activation for 4 min at 1.875 W/cm<sup>2</sup>. Dots show the mean values of  $n = 6$ .

### 2.2 Cell Death Effects of DTX Monotreatment.

To establish dose-response curves and EC<sub>50</sub> for DTX monotreatment, the percentage of cell death induced was determined after incubating the cells for 48-h with DTX concentrations ranging between 0.0025 - 20 nM, resulting in a dose-dependent increase in cell death [Figure 3]. Detroit 562 and FaDu were more sensitive to DTX at lower doses (1 nM and lower), whereas CAL 27 was most responsive to DTX at higher doses (2.5 nM and higher). The EC<sub>50</sub> values of DTX for Detroit 562, FaDu, and CAL 27 were 1.09 nM, 0.90 nM, and 1.24 nM, respectively [Table 1]. In the present study, 20 nM of DTX resulted

in approximately 94% cell death in Detroit 562 and FaDu and greater than 99% cell death in CAL 27 48 h after treatment.

**Table 1:** EC50 values for LANT and DTX monotreatments. The EC50 values informed the AuNRs concentrations and DTX doses used in the combination treatment.

EC50	Cell Lines		
	Detroit 562	FaDu	CAL 27
LANT (nM)	8.08	11.03	6.68
DTX (nM)	1.09	0.90	1.24

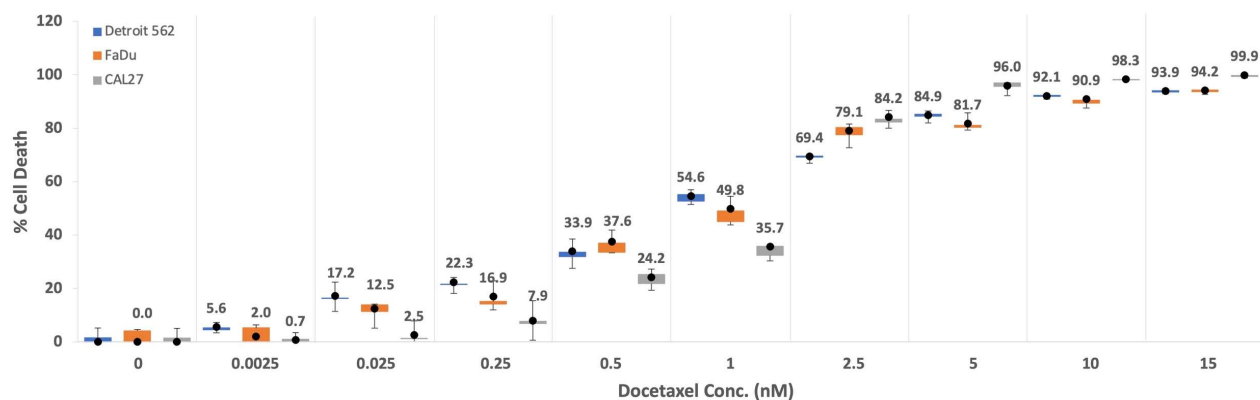


**Figure 3.** Box and Whisker plot to display DTX monotreatment dose-response with DTX concentration for HNSCC cell lines: Detroit 562 (blue box), FaDu (orange box), and CAL 27 (gray box). Mean percentage of cell death induced by a 48-h incubation with DTX as a monotreatment at 9 different concentrations of 0.0025, 0.025, 0.25, 0.5, 1, 2.5, 5, 10, and 15 nM for each cell line. Dots show the mean values of  $n = 6$ .

### 2.3 Combination of DTX and LANT Treatments.

Monotreatment EC50 values that induced 50% cell death [Table 1] informed the dose selection for the combination experiments to specifically narrow the focus to low doses for both DTX and LANT. To delineate and emphasize the efficacy of the DTX + LANT combination treatment, 0.5 and 1 nM of DTX were selected for the combination treatment as these concentrations induced less than 50% cell death for all cell lines. Likewise, 2.5 and 5 nM of AuNRs for LANT were selected as these concentrations induced less than 50% cell death for all cell lines. In general, the mean percentage of cell death generated by combining low dose DTX and low dose LANT is greater than the same low dose of DTX monotreatment. As shown in [Figure 4], the percentage of cell death due to the four DTX + LANT combination treatments, (DTX at 0.5 nM or 1 nM) + (LANT at 2.5 nM or 5 nM), was significantly higher than the two DTX monotreatments (0.5 nM or 1 nM) for all three HNSCC cell lines, Detroit 562, FaDu, and CAL 27.

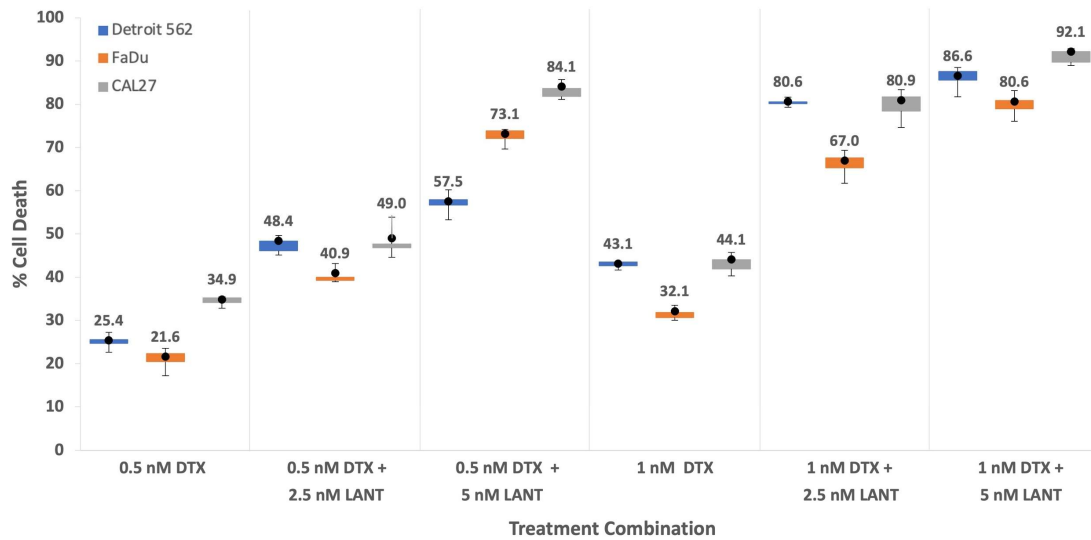


**Figure 4.** Box and Whisker plot to display LANT and DTX combination treatment for HNSCC cell lines: Detroit 562 (blue bar), FaDu (orange bar), and CAL 27 (gray bar), corresponding to Tables 2 and 3. Cells were subjected to a 48-h incubation with DTX at a concentration of 0.5 or 1 nM, as a monotreatment or combined with LANT at a concentration of 2.5 or 5 nM using NIR laser excitation for 4 min at 1.875 W/cm<sup>2</sup>. Dots show the mean values of n = 4.

**Table 2:** Therapeutic efficacy comparison of 15 treatment groups.

Treatment group comparison <sup>a</sup> (First Column vs. Second Column)		Detroit 562			FaDu			CAL 27		
		Mean	Unadj.	Adj.	Mean	Unadj.	Adj.	Mean	Unadj.	Adj.
		Diff. <sup>b</sup>	<i>p</i> -value <sup>c</sup>	<i>p</i> -value <sup>d</sup>	Diff. <sup>b</sup>	<i>p</i> -value <sup>c</sup>	<i>p</i> -value <sup>d</sup>	Diff. <sup>b</sup>	<i>p</i> -value <sup>c</sup>	<i>p</i> -value <sup>d</sup>
0.5 nM DTX + 2.5 nM LANT	0.5 nM DTX	23.0	<0.0001*	<0.0001*	19.3	<0.0001*	<0.0001*	14.2	<0.0001*	<0.0001*
0.5 nM DTX + 5 nM LANT	0.5 nM DTX	32.1	<0.0001*	<0.0001*	51.5	<0.0001*	<0.0001*	49.2	<0.0001*	<0.0001*
1 nM DTX + 2.5 nM LANT	0.5 nM DTX	55.2	<0.0001*	<0.0001*	45.3	<0.0001*	<0.0001*	46.1	<0.0001*	<0.0001*
1 nM DTX + 5 nM LANT	0.5 nM DTX	61.1	<0.0001*	<0.0001*	59.0	<0.0001*	<0.0001*	57.3	<0.0001*	<0.0001*
0.5 nM DTX + 2.5 nM LANT	1 nM DTX	5.3	0.0219	0.3285	8.8	0.0002 <sup>§</sup>	0.0036 <sup>§</sup>	4.9	0.0306	0.4595
0.5 nM DTX + 5 nM LANT	1 nM DTX	14.4	<0.0001*	<0.0001*	41.0	<0.0001*	<0.0001*	40.0	<0.0001*	<0.0001*
1 nM DTX + 2.5 nM LANT	1 nM DTX	37.5	<0.0001*	<0.0001*	34.8	<0.0001*	<0.0001*	36.9	<0.0001*	<0.0001*
1 nM DTX + 5 nM LANT	1 nM DTX	43.4	<0.0001*	<0.0001*	48.5	<0.0001*	<0.0001*	48.1	<0.0001*	<0.0001*
1 nM DTX	0.5 nM DTX	17.7	<0.0001*	<0.0001*	10.5	<0.0001*	0.0003	9.2	0.0001 <sup>§</sup>	0.0019 <sup>§</sup>
0.5 nM DTX + 5 nM LANT	0.5 nM DTX + 2.5 nM LANT	9.1	0.0001 <sup>§</sup>	0.0021 <sup>§</sup>	32.2	<0.0001*	<0.0001*	35.0	<0.0001*	<0.0001*
1 nM DTX + 2.5 nM LANT	0.5 nM DTX + 2.5 nM LANT	32.2	<0.0001*	<0.0001*	26.0	<0.0001*	<0.0001*	31.9	<0.0001*	<0.0001*
1 nM DTX + 5 nM LANT	0.5 nM DTX + 2.5 nM LANT	38.2	<0.0001*	<0.0001*	39.7	<0.0001*	<0.0001*	43.1	<0.0001*	<0.0001*
1 nM DTX + 2.5 nM LANT	0.5 nM DTX + 5 nM LANT	23.1	<0.0001*	<0.0001*	-6.2	0.0077	0.1157	-3.1	0.1658	0.999
1 nM DTX + 5 nM LANT	0.5 nM DTX + 5 nM LANT	29.0	<0.0001*	<0.0001*	7.5	0.0014 <sup>†</sup>	0.0204 <sup>†</sup>	8.1	0.0006 <sup>†</sup>	0.0097 <sup>†</sup>
1 nM DTX + 5 nM LANT	1 nM DTX + 2.5 nM LANT	5.9	0.0101	0.1522	13.7	<0.0001*	<0.0001*	11.2	<0.0001*	<0.0001*

<sup>a</sup> Comparing the therapeutic efficacy of each DTX monotreatment and combination treatment groups by the Linear Mixed Model (LMM) regression Post-Hoc tests with Bonferroni correction for three HNSCC

cell lines. For treatment group comparison, the first column was more effective than the second column by the mean difference amount.

<sup>b</sup> Mean Diff., Mean Difference = first column – second column

<sup>c</sup> Unadj. *p*-value, Unadjusted *p*-value; \* *p* < 0.0001; § *p* < 0.005; and † *p* < 0.05

<sup>d</sup> Adj. *p*-value, Adjusted *p*-value; \* *p* < 0.0001; § *p* < 0.005; and † *p* < 0.05

**Table 3**

DTX dose reduction percentage by DTX + LANT combination treatment.

Cell line	Outcome	Treatment combination			
		0.5 nM DTX + 2.5 nM LANT	0.5 nM DTX + 5 nM LANT	1 nM DTX + 2.5 nM LANT	1 nM DTX + 5 nM LANT
Detroit 562	Cell death (%) in combo	48.4	57.5	81.3	86.6
	Est. conc. (nM) of DTX mono to obtain the same % cell death	0.9	1.3	4.4	6.5
	DTX dose reduction (%)	43.0	61.7	77.2	84.6 <sup>a</sup>
FaDu	Cell death (%) in combo	40.9	73.1	67.0	80.6
	Est. conc. (nM) of DTX mono to obtain the same % cell death	0.6	2.3	1.7	3.5
	DTX dose reduction (%)	22.7	78.2 <sup>a</sup>	42.2	71.5
CAL 27	Cell death (%) in combo	49.0	84.1	80.9	92.1
	Est. conc. (nM) of DTX mono to obtain the same % cell death	1.2	2.8	2.6	4.2
	DTX dose reduction (%)	57.0	82.4 <sup>a</sup>	60.8	76.0

<sup>a</sup> Indicates the combination treatment that resulted in the highest percentage of DTX dose reduction for each cell line.

#### 2.4 Summary statistics and LMM regression post-hoc results.

The LMM regression post-hoc test compared the means of the six DTX and LANT monotreatments versus combination treatment groups for all three HNSCC cell lines according to our previously established methods [37]. These post-hoc analyses are summarized in Table 2, showing statistically significant differences (*p* < 0.05) in the means for most of the comparison groups. DTX and LANT treatment combinations were, in general, significantly more effective than the corresponding DTX monotreatments. In this study, the best-performing treatment regimen was the combination of 1 nM DTX + 5 nM LANT, with approximately an 86.6%, 80.7%, and 92.1% increase in cell death versus 1 nM DTX alone for Detroit 562, FaDu, and CAL 27 cells, respectively. The other treatment combinations also induced significantly more cell death than 0.5 or 1 nM DTX alone. There were 2 comparisons (of 15 comparison) for Detroit 562 and CAL 27 and 1 comparison for FaDu that did not reach statistical significance [Table 2].

The synergistic therapeutic efficacy accomplished by combining DTX and LANT (0.5 nM or 1 nM DTX + 2.5 nM or 5 nM LANT) and the percentage of DTX dose reduction was determined using the 4PL model equations according to our previously described methods [36,37]. Using the cell death percentage

induced by the DTX and LANT combination and the corresponding DTX monotreatment dose necessary to achieve the same cell death, we calculated the percentages of DTX dose reduction shown in Table 3. For Detroit 562, the largest DTX dose reduction was achieved by 1 nM DTX + 5 nM LANT combination treatment: 84.6%. The 0.5 nM DTX + 5 nM LANT combination treatment resulted in the highest percentage of DTX dose reduction for FaDu and CAL 27: 78.2% and 82.4%, respectively. For example, 86.6% Detroit 562 cell death can be induced by 6.5 nM of DTX monotreatment or 1 nM DTX when combined with 5nM LANT, demonstrating an 84.6% DTX dose reduction.

### 3 DISCUSSION

Adjuvant, neoadjuvant, and combination therapies are an emerging and viable approach to overcome the current challenges experienced by patients who cannot receive or tolerate standard chemotherapeutic treatment regimens. This *in vitro* study presents the possibility of a patient-centered solution that may reduce the standard DTX dosage, and thus may reduce associated side effects for patients with locally advanced HNSCC. DTX has shown promise to decrease toxicity at lower doses when combined with other therapeutic interventions while maintaining or improving efficacy.

Currently, the most widely accepted DTX combination therapy for HNSCC patients is cisplatin and 5-fluorouracil (TPF) [14,15]. This combination was found to effectively extend the survival rate in patients diagnosed with locally advanced HNSCC while reporting less toxicity-related deaths and side effects compared to cisplatin or cisplatin/5-fluorouracil (PF) alone [14,16]. Albers et al. demonstrated an effective and tolerable dosage of 75 mg/m<sup>2</sup> DTX on a 21-day cycle when combined with PF, a 25% decrease from the maximum tolerated dose of DTX as a single agent [40]. Other studies reveal improved outcomes with DTX dosage reduction, including a phase II clinical trial using DTX at 20 mg/m<sup>2</sup> per week combined with bevacizumab and radiotherapy. This combination showed promising survival outcomes despite a 40% decrease from the maximum standard dose of DTX [41].

Emerging preclinical and clinical studies combining DTX with novel interventions, like nanomedicines and therapeutic nanotechnologies, offer a renewed potential for DTX dose reduction and enhanced drug delivery [17,25-31,42,43]. A variety of nanomaterials have impacted DTX effectiveness by allowing for selective distribution to the cancer cells, increased circulation times, and a more sustained drug release [26-28]. Furthermore, surface-coated nanoparticles may significantly increase targeting, decrease immunogenicity, and suppress nonspecific binding to charged molecules [29-31]. Similar to our approach, Bannister et al. used PEGylated gold nanoparticles (GNPs) in tandem with DTX and radiotherapy as a therapeutic strategy, rather than a drug delivery system [17]. In their approach, DTX redistributed GNPs closer to the nucleus of cancer cells, enhancing DTX double-stranded breaks during radiation.

In this study, the treatment efficacy of combining LANT and DTX was assessed, and our results suggest that LANT improved the therapeutic efficacy of DTX *in vitro*. Our previous *in vivo* study showed that LANT monotreatment significantly induced tumor regression by approximately 100% ( $p < 0.0001$ ) with no observed side effects [33]. The performance of LANT monotreatment inspired the exploration of possibilities with DTX because lower DTX doses may ultimately result in fewer side effects and improved

patient outcomes. The scope of LANT is currently limited to a single, local treatment and therefore additional experimentation is needed to examine its potential application in recurrent and metastatic disease. Our future studies will address these limitations, validate our findings *in vivo*, and provide greater insight on the clinical implications of LANT and DTX combination treatment, including side effects and administration route. DTX and LANT combination treatment is designed to minimize the adverse effects of DTX as a synergistic therapeutic approach. Combining DTX + LANT increased the percentage of cell death by up to 3.4-fold, and the efficacy of cell death up to 51.5% more than DTX monotreatment. The most effective treatment combinations consistently demonstrated a > 80% dose reduction in DTX to achieve the same level of cell death as DTX alone. Our current results suggest that combining LANT with DTX may dramatically lower the dose necessary to achieve therapeutic efficacy. Future studies are needed to translate this *in vitro* concentration to an animal or human dose and verify clinical relevance.

## 4 MATERIALS AND METHODS

### 4.1 Materials

Gold (III) chloride trihydrate (HAuCl<sub>4</sub>), cetyltrimethylammonium bromide (CTAB), sodium borohydride (NaBH<sub>4</sub>), silver nitrate (AgNO<sub>3</sub>), L-ascorbic acid, potassium carbonate (K<sub>2</sub>CO<sub>3</sub>), and dimethyl sulfoxide (DMSO) were purchased from Sigma-Aldrich (St. Louis, MO). Thiol-terminated methoxy poly-(ethylene glycol) (mPEG-SH, MW 5,000K) and DTX were purchased from Creative PEGWorks (Winston-Salem, NC) and Selleck Chemicals (ImClone Systems, New York, NY), respectively. UltraPure water (18 MΩ) was used for gold nanorod preparation.

### 4.2 Preparation of AuNRs

AuNRs were prepared using seed-mediated growth, PEGylated, and characterized according to the gold nanorods fabrication and characterization methods previously reported [34]. Briefly, PEGylated AuNRs solution was centrifuged at 7,600 ×g for 20 min at 25°C and re-dispersed in deionized water to remove excess CTAB and non-specifically bound mPEG-SH molecules. The maximum peak of plasmon resonance absorption for different batches of AuNRs averaged at  $\lambda = 808$  nm as measured by a UV/VIS spectrophotometer UV5Nano (Mettler Toledo, LLC, Columbus, OH, USA). The shape and size of AuNRs were confirmed by an aberration-corrected dedicated Scanning Transmission Electron Microscope HF2000 STEM (Hitachi High-Tech Corporation, Tokyo, Japan). The AuNRs were approximately 40 nm by 10 nm, thus providing the aspect ratio,  $R = 4$ . The concentration of AuNRs was calculated using Beer-Lambert Law based on the previously determined molar absorptivity,  $\epsilon = 5 \times 10^9$  L • mol<sup>-1</sup> • cm<sup>-1</sup> for 808 nm and aspect ratio,  $R = 4$  [35].

### 4.3 Cell Lines

Human HNSCC cell lines, Detroit 562 (pharynx), FaDu (hypopharynx), and CAL 27 (tongue), were purchased from the American Type Culture Collection (ATCC, Manassas, VA). All are tumorigenic and can translate to *in vivo* studies using xenografted HNSCC mice models. Upon receiving the cell lines from ATCC, the passage number was set at one, and passage 3-7 of each cell line was used. Cells tested negative

for mycoplasma. Cells were cultured in Dulbecco's Modified Eagle Medium containing 10% v/v heat-inactivated fetal bovine serum, supplemented with 4.5 g/L glucose, L-glutamine, and penicillin-streptomycin, and incubated at 37°C with 5% CO<sub>2</sub>.

#### 4.4 Cell death by LANT and DTX monotreatments

For LANT monotreatment *in vitro*, a total of  $6 \times 10^4$  cells/well were seeded in 96-well culture plates and treated at approximately 100% confluence. The cell number per well was 6-times more than for DTX monotreatment to prepare a more than 99% confluent cell layer after seeding because the LANT effect is more immediate than anticancer drug cytotoxicity. AuNRs using a dose escalation of 0 – 25 nM in 25  $\mu$ L were added to each well and immediately exposed to a diode near-infrared (NIR) laser (Information Unlimited, Amherst, NH, USA) with 808 nm wavelength at 1.875 W/cm<sup>2</sup> (spot size around 4 x 4 mm<sup>2</sup>) for 4 min at room temperature. The 4-min duration of laser exposure *in vitro* was determined in our prior work [34] and used to maintain methodological consistency. Within 1 - 5 min after laser excitation of AuNRs, the percentage of cell death was determined by the PrestoBlue Assay according to the manufacturer's instructions. The percentage of cell death was calculated by subtracting the percentage of cell viability from 100% (see formula below).

$$\begin{aligned} \text{\% of cell death} &= 100 - \text{\% cell viability} \\ &= 100 - \frac{(\text{fluorescence of sample} - \text{fluorescence of blank})}{(\text{fluorescence of control} - \text{fluorescence of blank})} \times 100 \end{aligned}$$

For DTX monotreatment, cells were seeded in 96-wells plates at  $1 \times 10^4$  cells/well and allowed to adhere overnight. The culture medium was then replaced with a fresh medium containing DTX at various concentrations, 0.0025 - 20 nM, and cells were incubated at 37°C for 48 h. A pilot study was used to determine the ideal exposure time to DTX. The exposure for 24 h was not sufficient to induce cell death, and 72 h exposure induced too much cytotoxicity to distinguish the impact of LANT from the anticancer activity of the respective DTX dose. Therefore, 48 h exposure was selected as the ideal DTX treatment time for the combination with LANT. The percentage of cell death was determined by the PrestoBlue Assay. The half-effective concentrations (EC50) of DTX and LANT for the 3 HNSCC cell lines were calculated with the IC50 calculator provided by AAT Bioquest® using the Four-Parameter Logistic (4PL) model [36].

#### 4.5 Combination of DTX and LANT *in vitro*

HNSCC cells were treated with the combination of DTX and LANT according to the methods used in our previous study [37], adapted as follows: HNSCC cell lines were seeded in 96-well plates at  $1 \times 10^4$  cells/well and allowed to adhere overnight. The cell number was the same as that for DTX monotreatment. The culture medium was then replaced with fresh medium containing DTX at two concentrations (0.5 nM or 1 nM), and cells were incubated with DTX at 37°C for 48 h. Immediately after the 48-h incubation, the DTX-medium was removed, and the cells were washed with PBS once. Then 25  $\mu$ L of AuNRs in PBS at 2.5 nM or 5 nM were added onto the DTX-treated cells and exposed to 4 min of 808 nm wavelength NIR irradiation at 1.875 W/cm<sup>2</sup>. As described above, the final percentage of cell death induced by the DTX + LANT combination treatment was evaluated using the PrestoBlue Assay immediately after LANT

treatment. Each treatment combination was performed in quadruplicate ( $n = 4$ ), and the results are expressed as the mean  $\pm$  standard deviation.

The dose reduction realized by combining DTX with LANT was estimated by comparing the combination treatment to the monotreatment using the 4PL model equation for each cell line, as shown below.

For Detroit 562,

$$y = 5.955 + \frac{(100.971 - 5.955)}{1 + \left(\frac{x}{1.094}\right)^{-0.967}} \quad (\text{Equation 1a})$$

For FaDu,

$$y = 3.854 + \frac{(95.612 - 3.854)}{1 + \left(\frac{x}{0.895}\right)^{-1.197}} \quad (\text{Equation 1b})$$

For CAL 27,

$$y = 2.043 + \frac{(101.778 - 2.043)}{1 + \left(\frac{x}{1.238}\right)^{-1.842}} \quad (\text{Equation 1c})$$

To determine the percentage of cell death that is in common with both the DTX monotreatment and DTX + LANT combination treatment, we substituted the cell death percentage in the combination treatment obtained from real data for  $y$  in Eq. 1a - 1c for each cell line and then solved for  $x$  to calculate the corresponding DTX monotreatment dose.

#### 4.6 Statistical Power and Analysis

The total sample size for the regression analyses was 72 (four observations per each of the six treatments ( $n = 6$ ) and three cell lines). We assumed (1) an Ordinary Least Square multiple regression model with the treatment by cell lines as predictors, (2) an assumed  $R^2$  value of 0.7 for the full model (proportion of variability in percent cell death explained by the treatment by cell combinations), (3) a differential effect in  $R^2$  of 0.025 for each treatment by cell line combination, and (4) overall 0.05 significance level. Consequently, there is at least 90% power to detect a statistically significant difference between at least eight comparisons of DTX and LANT versus DTX monotreatment. Cell death percentages across the six treatment conditions, by cell line, were summarized by mean and standard deviations, median (min and max). Comparisons in percent cell death between treatment combinations by cell lines were undertaken using Linear Mixed Model (LMM) regression modeling approach with interaction (between treatment and cell lines) terms. Multiple comparisons were adjusted using the Bonferroni correction, with an overall nominal statistical significance of  $\alpha = 0.05$ . No sigmoid (non-linear) feature for data was detected since all of the percent data lies between 17-95. However, given the bounded nature of the percent data (between 0 and 100), LMM results were also confirmed using a two-limit Tobit model [38]. The comparisons of interest are those between DTX monotreatment (i.e., 0.5 nM DTX and 1 nM DTX) and DTX and LANT combination treatment (i.e., 0.5 nM DTX + 2.5 nM LANT; 0.5 nM DTX

+ 5 nM LANT; 1 nM DTX + 2.5 nM LANT; and 1 nM DTX + 5 nM LANT). Summaries and differences were plotted using Boxplots. All analyses used SAS 9.4 and R statistical software (R Core Team, 2019).

## ACKNOWLEDGEMENTS

The authors would like to thank the supporters and volunteers at the Ora Lee Smith Cancer Research Foundation for their endeavors to translate LANT from bench to bedside, while making it affordable and accessible. This study was primarily supported by the Biomedical Laboratory Research and Development Service of the VA Office of Research and Development [I01BX007080]; and partially supported by the National Center for Advancing Translational Sciences of the National Institutes of Health [UL1TR000454]; and National Cancer Institute [grant numbers P30CA013148, P50CA098252, U54CA118938, U54CA118623, and U54CA118948]. The authors disclose the following patent as a potential conflicts of interest: Green, H.N. Photothermal nanostructures in tumor therapy. U.S. Patent No. US 9,827,441 B2. (Issued Nov 28, 2017).

## AUTHOR CONTRIBUTION

Gee Young Lee: Conceptualization; Data curation; Investigation; Methodology; Validation, Visualization; Writing – Original Manuscript Preparation and Revisions. Mohamed Mubasher: Formal analysis. Tamra McKenzie: Writing-review & editing. Nicole C. Schmitt: Writing-review & editing. Merry E. Sebelik: Writing – Review & Editing. Carrie E. Flanagan: Writing – Review & Editing. Maya B. Cothran: Writing – Original Draft Preparation. Hadiyah N. Green: Conceptualization (equal); Data analysis; Funding acquisition; Methodology; Project administration; Resources; Supervision; Writing – Original Manuscript Preparation and Revisions.

## Data Statement

The datasets used and/or analyzed during the current study are available from the corresponding author on reasonable request.

## References

1. Siegel R, Naishadham D, Jemal A. Cancer statistics, 2013. *CA Cancer J Clin* 2013;63:11–30. doi:10.3322/caac.21166
2. Bray F, Ferlay J, Soerjomataram I, et al. Global cancer statistics 2018: GLOBOCAN estimates of incidence and mortality worldwide for 36 cancers in 185 countries. *CA Cancer J Clin* 2018;68:394–424. doi:10.3322/caac.21492
3. Blanchard P, Baujat B, Holostenco V, et al. MACH-CH Collaborative group. Meta-analysis of chemotherapy in head and neck cancer (Mach-Ne): A comprehensive analysis by tumour site. *Radiother Oncol* 2011;100:33–40. doi:10.1016/j.radonc.2011.05.036
4. Vigneswaran N, Williams MD. Epidemiologic trends in head and neck cancer and aids in diagnosis. *Oral Maxillofac Surg Clin North Am* 2014;26:123–41. doi:10.1016/j.coms.2014.01.001

5. Marur S, Forastiere AA. Head and neck squamous cell carcinoma: update on epidemiology, diagnosis, and treatment. *Mayo Clin Proc* 2016;91:386–396. doi:10.1016/j.mayocp.2015.12.017
6. Alsahafi E, Begg K, Amelio I, et al. Clinical update on head and neck cancer: Molecular biology and ongoing challenges. *Cell Death Dis* 2019;10:540. doi:10.1038/s41419-019-1769-9
7. Docetaxel - national cancer institute. Published May 10, 2006. Accessed March 2, 2021. <https://www.cancer.gov/about-cancer/treatment/drugs/docetaxel>
8. Lyseng-Williamson KA, Fenton C. Docetaxel: A review of its use in metastatic breast cancer. *Drugs* 2005;65:2513–2531. doi:10.2165/00003495-200565170-00007
9. McKeage K. Docetaxel: A review of its use for the first-line treatment of advanced castration-resistant prostate cancer. *Drugs* 2012;72:1559–1577. doi:10.2165/11209660-000000000-00000
10. Ho MY, Mackey JR. Presentation and management of docetaxel-related adverse effects in patients with breast cancer. *Cancer Manag Res* 2014;6:253–259. doi:10.2147/CMAR.S40601
11. Marur S, Forastiere AA. Head and neck squamous cell carcinoma: Update on epidemiology, diagnosis, and treatment. *Mayo Clin Proc* 2016;91:386–396. doi:10.1016/j.mayocp.2015.12.017
12. Bernier J, Vrieling C. Docetaxel in the management of patients with head and neck squamous cell carcinoma. *Expert Rev Anticancer Ther* 2008;8:1023–1032. doi:10.1586/14737140.8.7.1023
13. Haddad RI, Posner M, Hitt R, et al. Induction chemotherapy in locally advanced squamous cell carcinoma of the head and neck: Role, controversy, and future directions. *Ann Oncol* 2018;29:1130–1140. doi:10.1093/annonc/mdy102
14. DailyMed - DOCETAXEL injection, solution. <https://dailymed.nlm.nih.gov/dailymed/drugInfo.cfm?setid=3104aab1-cd6e-4ad2-8e0a-286a0c5d1940#S5.1>. Accessed March 2, 2021.
15. Albers AE, Grabow R, Qian X, et al. Efficacy and toxicity of docetaxel combination chemotherapy for advanced squamous cell cancer of the head and neck. *Mol Clin Oncol* 2017;7:151–157. doi:10.3892/mco.2017.1281
16. Galletti E, Magnani M, Renzulli ML, et al. Paclitaxel and docetaxel resistance: Molecular mechanisms and development of new generation taxanes. *Chem Med Chem* 2007;2:920–942. doi:10.1002/cmdc.200600308
17. Bannister AH, Bromma K, Sung W, et al. Modulation of nanoparticle uptake, intracellular distribution, and retention with docetaxel to enhance radiotherapy. *Br J Radiol* 2020;93:20190742. doi:10.1259/bjr.20190742
18. Tran PHL, Duan W, Lee BJ, et al. Nanogels for skin cancer therapy via transdermal delivery: Current designs. *Curr Drug Metab* 2019;20:575–582. doi:10.2174/1389200220666190618100030
19. Her S, Jaffray DA, Allen C. Gold nanoparticles for applications in cancer radiotherapy: Mechanisms and recent advancements. *Adv Drug Deliv Rev* 2017;109:84–101. doi:10.1016/j.addr.2015.12.012
20. Essawy MM, El-Sheikh SM, Raslan HS, et al. Function of gold nanoparticles in oral cancer beyond drug delivery: Implications in cell apoptosis. *Oral Dis*. 2021;27:251–265. doi:10.1111/odi.13551
21. Choi YJ, Kim YJ, Lee JW, et al. Cytotoxicity and genotoxicity induced by photothermal effects of colloidal gold nanorods. *J Nanosci Nanotechnol* 2013;13:4437–4445. doi:10.1166/jnn.2013.7176

22. Zhou B, Song J, Wang M, et al. BSA-bioinspired gold nanorods loaded with immunoadjuvant for the treatment of melanoma by combined photothermal therapy and immunotherapy. *Nanoscale* 2018;10:21640–21647. doi:10.1039/c8nr05323e
23. Hijaz M, Das S, Mert I, et al. Folic acid tagged nanoceria as a novel therapeutic agent in ovarian cancer. *BMC Cancer* 2016;16:220. doi:10.1186/s12885-016-2206-4
24. Li H, Qu X, Qian W, et al. Andrographolide-loaded solid lipid nanoparticles enhance anti-cancer activity against head and neck cancer and precancerous cells. *Oral Dis*. Published online December 9, 2020. doi:10.1111/odi.13751
25. Sun B, Feng SS. Trastuzumab-functionalized nanoparticles of biodegradable copolymers for targeted delivery of docetaxel. *Nanomedicine (Lond)* 2009;4:431–445. doi:10.2217/nmm.09.17
26. Tang X, Wang G, Shi R, et al. Enhanced tolerance and antitumor efficacy by docetaxel-loaded albumin nanoparticles. *Drug Deliv* 2016;23:2686–2696. doi:10.3109/10717544.2015.1049720
27. Bowerman CJ, Byrne JD, Chu KS, et al. Docetaxel-loaded PLGA nanoparticles improve efficacy in taxane-resistant triple-negative breast cancer. *Nano Lett* 2017;17:242–248. doi:10.1021/acs.nanolett.6b03971
28. Choudhury H, Gorain B, Pandey M, et al. Recent advances in TPGS-based nanoparticles of docetaxel for improved chemotherapy. *Int J Pharm* 2017;529:506–522. doi:10.1016/j.ijpharm.2017.07.018
29. Wan J, Ma X, Xu D, et al. Docetaxel-decorated anticancer drug and gold nanoparticles encapsulated apatite carrier for the treatment of liver cancer. *J Photochem Photobiol B* 2018;185:73–79. doi:10.1016/j.jphotobiol.2018.05.021
30. Chi C, Li F, Liu H, et al. Docetaxel-loaded biomimetic nanoparticles for targeted lung cancer therapy *in vivo*. *J Nanopart Res* 2019;21:144. doi:10.1007/s11051-019-4580-8
31. Ahmad T, Sarwar R, Iqbal A, et al. Recent advances in combinatorial cancer therapy via multifunctionalized gold nanoparticles. *Nanomedicine (Lond)* 2020;15:1221–1237. doi:10.2217/nmm-2020-0051
32. Popp MK, Oubou I, Shepherd C, et al. Photothermal therapy using gold nanorods and near-infrared light in a murine melanoma model increases survival and decreases tumor volume. *J Nanomater* 2014;2014:Article ID 450670. doi:10.1155/2014/450670
33. Green HN, Crockett SD, Martyshkin DV, et al. A Histological evaluation and *in vivo* assessment of intratumoral near infrared photothermal nanotherapy-induced tumor regression. *Int J Nanomed* 2014;9:5093–5102. doi:10.2147/IJN.S60648
34. Green HN, Martyshkin DV, Rosenthal EL, et al. A minimally invasive multifunctional nanoscale system for selective targeting, imaging, and NIR photothermal therapy of malignant tumors. In: SPIE BiOs. Achilefu S, Raghavachari R, eds.; 2011:79100B. doi:10.1117/12.875792
35. Link S, El-Sayed MA. Simulation of the optical absorption spectra of gold nanorods as a function of their aspect ratio and the effect of the medium dielectric constant. *J Phys Chem B* 2005;109:10531–10532. doi.org/10.1021/jp058091f
36. Sebaugh JL. Guidelines for accurate EC50/IC50 estimation. *Pharm Stat* 2011;10:128–134. doi:10.1002/pst.426

37. Lee GY, Mubasher M, Pollack BP, et al. Combination paclitaxel and Laser-Activated NanoTherapy for inducing cell death in head and neck squamous cell carcinoma. *J Nanomed & Nanotech* 2021;12:557.
38. Long JS. *Regression Models for Categorical and Limited Dependent Variables*. Thousand Oaks: Sage Publications; 1997.
39. Lee GY, Myers JA, Perez SM, et al. Cisplatin combined with laser-activated nanotherapy as an adjuvant therapy for head and neck cancer. *Int J Oncol* 2020;57:1169–1178. doi:10.3892/ijo.2020.5126
40. Figgitt DP, Wiseman LR. Docetaxel: An update of its use in advanced breast cancer. *Drugs* 2000;59:621–651. doi:10.2165/00003495-200059030-00015
41. Yao M, Galanopoulos N, Lavertu P, et al. Phase II study of bevacizumab in combination with docetaxel and radiation in locally advanced squamous cell carcinoma of the head and neck. *Head Neck* 2015;37:1665–1671. doi:10.1002/hed.23813
42. Adkins D, Ley J, Atiq O, et al. Nanoparticle albumin-bound paclitaxel with cetuximab and carboplatin as first-line therapy for recurrent or metastatic head and neck cancer: A single-arm, multicenter, phase 2 trial. *Oral Oncology* 2021;115:105173. doi:10.1016/j.oraloncology.2020.105173
43. Marcazzan S, Varoni EM, Blanco E, et al. Nanomedicine, an emerging therapeutic strategy for oral cancer therapy. *Oral Oncology* 2018;76:1-7. doi:10.1016/j.oraloncology.2017.11.014